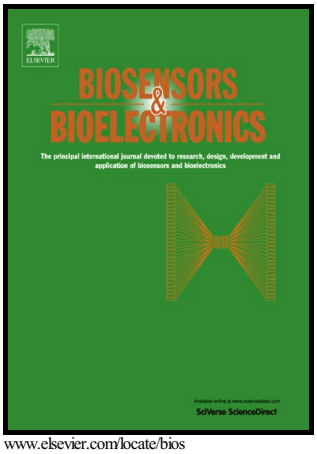

www.elsevier.com/locate/bios

Fabrication of Mediator-Free Hybrid Nano-Interfaced Electrochemical Biosensor for Monitoring Cancer Cell Proliferation

Madhurantakam Sasya, K. Jayanth Babu, John Bosco Balaguru Rayappan, Uma Maheswari Krishnan

PII: S0956-5663(16)30915-0
DOI: http://dx.doi.org/10.1016/j.bios.2016.09.039
Reference: BIOS9151

To appear in: *Biosensors and Bioelectronic*

Received date: 14 June 2016
Revised date: 8 September 2016
Accepted date: 10 September 2016

Cite this article as: Madhurantakam Sasya, K. Jayanth Babu, John Bosc Balaguru Rayappan and Uma Maheswari Krishnan, Fabrication of Mediator-Fre Hybrid Nano-Interfaced Electrochemical Biosensor for Monitoring Cancer Cel P r o l i f e r a t i o n , *Biosensors and Bioelectronic* http://dx.doi.org/10.1016/j.bios.2016.09.039

Fabrication of Mediator-Free Hybrid Nano-Interfaced Electrochemical Biosensor for Monitoring Cancer Cell Proliferation

Madhurantakam Sasya[1], Jayanth Babu K[2], John Bosco Balaguru Rayappan[1,2], Uma Maheswari Krishnan[1]*

[1] Centre for Nano Technology & Advanced Biomaterials (CeNTAB),

[2] School of Electrical & Electronics Engineering,

SASTRA University

Thanjavur – 613 401, India

*Corresponding Author

Prof. Uma Maheswari Krishnan Ph. D.

Deakin Indo–Australia Chair Professor

Associate Dean for the Departments of Chemistry, Bioengineering & Pharmacy

Centre for Nanotechnology & Advanced Biomaterials (CeNTAB)

School of Chemical & Biotechnology

SASTRA University, Thanjavur – 613 401

Tamil Nadu, India.

Ph.: (+91) 4362 264101 Ext: 3677

Fax: (+91) 4362 264120

E–mail: umakrishnan@sastra.edu

Abstract

Glucose, a chief energy source in cellular metabolism, has a significant role in cell proliferation. Cancer cells utilize more glucose than normal cells to meet the energy demand arising due to their uncontrolled proliferation. The present work reports the

development of a nano-interfaced amperometric biosensor for rapid and accurate monitoring of glucose utilization by cancer cells. A hybrid nano-interface comprising a blend of carbon nanotubes (CNTs) and graphene (GR) was employed to enhance the surface area of the working electrode and favour direct electron transfer. Glucose oxidase (GOx) immobilized on the interface serves as the sensing element due to its high selectivity and sensitivity towards glucose. Utilization of glucose was monitored at pre-determined time intervals in MiaPaCa-2 cancer cells. The results obtained from the amperometric technique were compared with the values obtained from a commercial glucometer. Alamar blue assay was performed to check the proliferation rate of the cells. A good correlation was obtained between the proliferation rate and glucose utilization. The designed biosensor was found to be unaffected by the presence of potential interferents and hence may serve as a novel *in vitro* tool to rapidly quantify the proliferation rates of cancer cells in response to different treatment strategies.

Keywords:

Hybrid nano interface, electrochemical biosensor, cancer cell proliferation, glucose sensor

1. Introduction

Cancer is a disease characterized by unregulated proliferation of cells and existence of altered metabolic pathways (Coller et al., 2015; Griss et al., 2015). If glucose levels exceed physiological concentrations (5.5 mM), it results in altered metabolism due to a phenomenon known as Warburg effect that promotes migration, proliferation and adhesion of cancer cells (Klement and Kämmerer, 2011; Masur et al., 2011). The energy demand of the rapidly proliferating cancer cells results in higher glucose consumption when compared with normal cells (Jang et al., 2013; Zheng, 2012). A pictorial representation of glucose metabolism in normal and cancer cells is provided in Supplementary figure 1. Evaluation of the efficacy of anti-cancer agents to inhibit cancer cell proliferation involves monitoring cell proliferation. Conventional methods for

determining cell proliferation employ dyes like Alamar blue, tetrazolium salts, lactate dehydrogenase and BrdU (Korzeniewski and Callewaert, 1983; Kulldorff et al., 2000; Rampersad, 2012; Skehan et al., 1990). These assays typically quantify the metabolically active cells and do not provide accurate measure of the quiescent cells. All these conventional methods involve long analysis time and expensive reagents. Moreover, many of these assays cannot be used for time-dependent monitoring of cells owing to the cytotoxicity of the reagents involved. Other limitations include non-compatibility with certain cell types and variations in assay responsiveness due to pH, buffers, incubation temperature, light sensitivity, cell density etc. (Rampersad, 2012). In this context, we propose to explore the feasibility of employing glucose utilization measurements for determining the proliferation rate of cells using a nano-interfaced electrochemical biosensor.

Electrochemical sensors possess several unique features like quick response, simple instrumentation, low cost, easy preparation, good selectivity, high specificity and sensitivity (Li et al., 2015; Suneesh et al., 2013). Glucose oxidase (GOx), a glucose-specific enzyme has been extensively used in electrochemical biosensors for the detection of glucose (Hu et al., 2015; Hyun et al., 2014; Kang et al., 2009; Zhang et al., 2011). GOx contains a flavin adenine dinucleotide (FAD) coenzyme and iron co-factor. The FAD is deeply buried in the protein shell, which reduces the electron transfer rate between the active site of the enzyme and surface of the electrode (Wang et al., 2011). Use of a nano-dimensional interface can facilitate direct electron transfer from the enzyme to the electrode surface resulting in subsequent improvement in surface area and response time (Gopalan et al., 2009). A wide variety of nanomaterials such as metals (Fu et al., 2014), metal oxides (Felix et al., 2014; Lei et al., 2010; Panky et al., 2013; Si et al., 2011; Suneesh et al., 2013), carbon-based structures (Zhu et al., 2010) and quantum dots (Zhao et al., 2011) have been explored as single interfaces in electrochemical biosensors.

Recently, the field of electrochemical biosensors has witnessed a paradigm shift with the emergence of hybrid nano-interfaces on the electrode surface. These hybrid interfaces integrate the positive aspects of the constituent nanoparticles and hence can enhance the sensor performance. Bimetallic compounds namely Cu-Ag (Li et al., 2015), NiO-SiC (Yang et

al., 2015), Pt-CNT (Yang et al., 2012), NiO-GR (Li et al., 2014), metal-polymer hybrids like Ag-PVA (Guascito et al., 2011), CuNPs-P3MT (Malitesta et al., 2013) and CuO-GR-CNF (Ye et al., 2013) have been used in the designing of electrochemical biosensors. CNTs and GR have been independently employed as interface materials owing to their superior electrical and mechanical properties. Both nanomaterials have demonstrated good biocompatibility, thermal stability, high surface area-to-volume ratio, enable greater entrapment of biomolecules, facilitate high electron transfer and are inert towards the entrapped biomolecules. They have also been reported to reduce the overpotential (Sun et al., 2011; Zhang et al., 2014). Hybrid interface of CNT-GR has been recently explored for aptamer-based detection of cardiac myoglobin (Kumar et al., 2015). In the present study, we have focused on the use of CNT-GR hybrid interface coupled with GOx to improve the sensing characteristics of the electrochemical glucose biosensor for monitoring cancer cell proliferation. To the best of our knowledge, no prior reports are available on sensors for monitoring cancer cell proliferation based on glucose utilization.

2. Materials and methods

2.1. Materials

D-Glucose (Hi-media, India), glucose oxidase, nafion (Sigma-Aldrich Ltd., USA), multi-walled carbon nanotubes (Nanoamor, USA), graphene (Redex Nano Lab, India), sodium hydroxide, potassium dihydrogen phosphate, dipotassium hydrogen phosphate, acetic acid, ascorbic acid, citric acid and uric acid (Merck, India) were used in the study. Ag/AgCl reference electrode (CHI111, 0.5 mm diameter), glassy carbon electrode (GCE, CHI102, 2 mm diameter) and platinum wire counter electrode (CHI115, 0.5 mm diameter) were purchased from CH Instruments, Inc., USA. MiaPaCa-2 pancreatic cancer cell line was procured from NCCS, Pune. Dulbecco's modified Eagles' medium (DMEM), phosphate-buffered saline (PBS), fetal bovine serum (FBS), Penicillin/streptomycin, trypsin (0.05%) were purchased from Gibco, USA. Cell viability studies were performed using Alamar blue assay kit (Promega, USA). All solutions and reagents were prepared using deionized water.

2.2. Characterization of CNT-GR mixture

Raman spectrum (Labram HR-800) was recorded to confirm the presence of both CNTs and graphene (GR) in the hybrid interface. Raman spectra were recorded between 0 to 1500 cm^{-1} for all the interface materials. Morphology of the samples was investigated using field emission scanning electron microscopy (FE-SEM, JSM 6701F, Japan). The samples were sputter-coated with a thin layer of gold prior to imaging.

2.3. Modification of working electrode

The glassy carbon electrode was cleaned with alumina slurry of different sizes (1µ, 0.3µ, 0.05µ) and then sonicated with ethanol and double distilled water. CNTs, GR and 1:1 mixture of CNTs and GR dispersed in 0.05 % nafion solution were sonicated in separate tubes for 1 h. Glucose oxidase enzyme solution was then added named as CNT-GR-GOx. 3µL of CNT-GR-GOx solution was coated on the GCE surface, dried for 1 h and denoted as GCE/CNT-GR-GOx (Supplementary figure 2). Similarly, 3 µL of CNTs, 3 µL of GR, 3 µL of CNT-GR solutions were drop cast on the glassy carbon electrode and denoted as GCE/CNT, GCE/GR and GCE/CNT-GR respectively.

2.4. Electrochemical measurements

Electrochemical studies were performed using electrochemical workstation (CHI 6013C, CH Instruments, USA) with three-electrode system. Ag/AgCl (saturated with 1M KCl) was used as a reference electrode, platinum wire as counter electrode and modified glassy carbon electrode (GCE/CNT/GR/GOx) was used as working electrode. Cyclic voltammetry and amperometric i-t curves were recorded in 10mL PBS (0.1M, pH 7.4).

2.5. Sample preparation and cell culture studies

MiaPaCa-2 cells were cultured in a CO_2 incubator at 37^{o}C and supplemented with DMEM containing 10% FBS, 1% penicillin/streptomycin. Confluent cells were seeded in a 96-well plate with different seeding densities varying from 1000 to10000 cells (n=3), and incubated for the adhesion of cells. After 24 h, the medium was replaced with fresh medium. At pre-determined time points, the spent medium was used for electrochemical studies. The same sample was subjected to Alamar blue assay following standard protocol

to quantify cell proliferation (Supplementary data). The cells were stained with tryphan blue and counted using hemocytometer to obtain the cell numbers for comparison.

3. Results and discussion

3.1. Characterization of the MWCNT-graphene interface

3.1.a. Raman spectroscopy

Raman spectroscopy was employed to obtain both qualitative and quantitative information on the structure and purity of MWCNTs, graphene and MWCNT-graphene mixture and the results are shown in figure 1(G). A low intense D band was observed for MWCNTs at 1320 cm^{-1} and a higher intensity G band appeared at 1573 cm^{-1}, which is typical for MWCNTs. The G-band arises due to the in-plane vibrations of the C-C bond while the D-band is disorder-induced (Bokobza and Zhang, 2012). A small but detectable radial breathing mode arising due to bond stretching out-of-plane phonon mode and resonant scattering is observed at 253 cm^{-1} that provides additional confirmation for the presence of small diameter MWCNTs. Raman spectrum of GR showed an intense D-band around 1323 cm^{-1} and a less intense G-band at 1584 cm^{-1}. The D band indicates presence of defects in the graphene structure. The G band due to the in-plane vibrations of sp^2 carbon appears in the range reported earlier for 2-D graphene. The intensity ratio of I_d/I_g was found to be 2.33 which is in the range reported for pure graphene (Childres et al., 2013; Zhou et al., 2010).

MWCNT-graphene showed two distinct peaks at 1320 cm^{-1} (D-band) and 1579 cm^{-1}(G-band). The I_d/I_g ratio of the mixture was 2.29. The upfield shift in the G-band of the mixture with respect to that of the pristine MWCNTs suggests disentanglement of the CNT tubes arising due to the addition of graphene. On the other hand, when compared with the Raman spectrum of pristine graphene, the mixture exhibited a downfield shift of the G-band suggesting an increase in the thickness of the graphene layers. This may arise due to the intercalation of CNT within the graphene sheets. The increase in the intensity of the D-band at 1320 cm^{-1} is associated with introduction of defects or other chemical species to the walls of the CNT (Song et al., 2016).

3.1.b. Scanning Electron microscopy

The scanning electron micrographs of the pristine and composite structures are presented in Figure 1(A-F). The scanning electron micrograph of MWCNTs (Figure 1A) reveals a mesh-like network of uniform sized nanotubes while the layered arrangement of graphene sheets are clearly discernible in Figure 1B. The physical admixture of MWCNTs and graphene reveals the presence of both phases (Figure 1C) while in the presence of the anionic nafion, a more intimate mixture of the two components was observed with nearly indistinguishable phases of CNTs and GR (Figure 1D). Post-addition of the glucose oxidase enzyme, a uniform distribution of all three components is observed (Figure 1 E&F) which augers well for sensing applications.

3.2. Electrochemical studies

3.2.a. Cyclic voltammetry

The influence of the different types of electrode modifications and nanointerfaces on the electrochemical parameters of the system was investigated by performing cyclic voltammetry in the potential range of -0.7 V to 0 V at the scan rate of 0.01 Vs^{-1}. Different modified electrodes were investigated and the results are presented in Figure 2A. The MWCNT-modified electrode showed a current value of 11.77 μA at a potential of -0.261 V. Modification of the electrode with graphene resulted in higher current values (18.92 μA) when compared to MWCNT interface. This is on expected lines as graphene sheets have been demonstrated to exhibit better electrical conductivity when compared with MWCNTs (Du et al., 2011; Marinho et al., 2012). When the electrode surface was modified with a 1:1 mixture of MWCNT and graphene, a reduction in the current to 9.11 μA was observed. This may be attributed to the disruption of the continuous sheets of graphene by the incorporation of CNTs. Further, the cyclic voltammograms of MWCNT-interfaced and GR-interfaced electrodes reveal large ΔEp values of 104 mV and 180 mV respectively. This indicates the irreversible nature of the reactions at these interfaces. The CNT/GR hybrid interface exhibited a lower ΔEp value of 78 mV indicating better overall conductivity of the CNT/GR mixture. The choice of the interface for immobilization of the glucose oxidase enzyme was based on the surface area measurements. Enhanced adsorption of the substrate on the electrode will increase the current flow. The surface coverage (Γ) for

glucose adsorption on various modified GCE electrodes were calculated using the following equation:

$$\text{Surface coverage } (\Gamma) = \frac{Q}{nFA}$$

where 'Q' is the charge, 'n' is the number of electrons transferred, 'F' is the Faraday constant (96500 C) and 'A' is the area of the electrode.

The CNT/GR hybrid interface showed a significant enhancement in the surface area of electrode with 25.24 x 10^{-9} cm^2, which was found to be 3-fold higher than those calculated for pristine MWCNT and graphene interfaces. Both the surface coverage as well as consumption of charge is high in the CNT/GR hybrid interface. Thus, it is possible that CNT/GR hybrid interface can enhance the sensor performance when compared with the single interfaces. Glucose oxidase (GOx) enzyme was introduced in to the hybrid interface to achieve specificity towards glucose. This modified electrode was represented as GCE/CNT-GR-GOx. The current response in the cyclic voltammogram of GCE/CNT-GR-GOx electrode in the absence and presence of 1 mM glucose was shown in Figure 2 (B). The anodic and cathodic peak potentials at a scan rate of 0.01V/s are observed at -0.443V and 0.503V respectively. The appearance of these peaks is consistent with earlier reports and can be attributed to the reduction and oxidation of FAD/$FADH_2$ electroactive centre of the GOx enzyme by direct electron transfer (Guo and Li, 2010; Kang et al., 2007; Lyons and Keeley, 2006; Wu et al., 2009). The reaction mechanism is represented below

$$GOx(FAD) + 2H + 2\,e^- \rightleftharpoons GOx(FADH_2)$$

The cyclic voltammogram of CNT-GR-GOx in the presence of 1 mM of glucose shows lower $\Delta \boldsymbol{Ep}$ of 60 mV when compared to the CNT/GR hybrid interface in the absence of glucose. The current flowing through the system also exhibited a considerable increase to 12.93 µA. High conductivity and rapid one-electron transfer with low operating working potential was obtained on the GOx modified electrode in the presence of glucose. The active surface coverage for adsorption of glucose on GCE/CNT-GR-GOx was also found to be 1.5 fold higher than on GCE/CNT-GR, which indicates the greater adsorption of glucose on to the redox center of GOx. Both oxidation and reduction peaks are discernible in the enzyme-

modified electrode with CNT-GR hybrid interface. Details of peak potential value, shift in peak current and surface coverage of all the modified electrodes are summarized in Supplementary table 1.

In order to assess the stability of the modified GCE/CNT-GR-GOx electrode, cyclic voltammetry was performed for about 20 sweep segments in the presence of glucose (Supplementary figure 3). It was observed that there is no significant change in the peak oxidation potential. The corresponding current values also did not exhibit large changes with a variation well below 1.5 μA in the presence of glucose. These results confirm the stability and reproducibility of the data obtained from the modified GCE/CNT-GR-GOx electrode.

Figure 2(D) depicts the cyclic voltammograms recorded for the GCE/CNT-GR-GOx in the presence of 1mM glucose at various scan rates ranging from 0.01 Vs^{-1} to 0.1 Vs^{-1}. A progressive increase in both the oxidation and reduction peaks was observed with increasing scan rates. The sensing phenomenon can either be surface-confined or diffusion-confined. These can be defined based on the relationship between the scan rate and peak current values in the cyclic voltammograms. The cathodic and the anodic peak currents increased linearly (R^2 = 0.995) with the scan rate ranging from 0.01Vs^{-1} to 0.1 Vs^{-1} (Figures 2D, 2E & 2F) that clearly indicates a surface-controlled electron transfer process rather than a diffusion-controlled process. This clearly indicates the surface controlled sensing nature of the designed biosensor.

We also investigated the reversibility of the reaction mechanism based on the cyclic voltammograms. The difference between oxidation (Epa) and reduction (Epc) peak potentials denoted as $\Delta \boldsymbol{Ep}$ was calculated as 60 mV. According to the Nernst equation, reactions with $\Delta \boldsymbol{Ep}$ greater than 59 mV are classified as quasi-reversible and hence the reaction at the GCE/CNT-GR/GOx is quasi-reversible. The average peak potential of anodic and cathodic peak potential was found to be -0.47 V at pH 7.4 which is similar to the reported standard reduction potential of GOx bound FAD (-0.46 at pH 7). The slight shift from standard potential to -0.47 V in the reduction potential may be due to the increase in

the pH from 7 to 7.4. This again confirms that the reaction occurs due to the FAD centre present in GOx (Hyun et al., 2014; Kang et al., 2009; Liu and Ju, 2003; Periasamy et al., 2011).

To check the concentration dependency of the designed GCE/CNT-GR-GOx biosensor, cyclic voltammetry was performed at a scan rate of 0.1 Vs^{-1} in PBS for increasing concentrations of glucose. As the concentration of glucose was increased from 1 mM to 7 mM, a gradual decrease in the both reduction and oxidation peak currents was observed (Figure 2G). This decrease in the oxidation and reduction currents was due to increase in the O_2 consumption at the electrode. A slight shift in the peak potentials was observed due to electron transfer limitation (Dantas et al., 2014). The plot of peak current versus concentration of glucose exhibited linearity from 1 mM to 7mM with a regression coefficient of 0.93 indicating surface-confined reactions (Figure 2H).

3.2.b. Amperometric detection of glucose

Amperometry was performed at the optimal potential of -0.45 V ((Epa+Epc)/2) after addition of equal increments of glucose to 10 mL PBS at pH 7.4 and the results are presented in Figure 3. A step-wise decreasing pattern was observed for successive additions of glucose. This decrease in current may be attributed to the consumption of electrons by O_2 during the enzymatic reaction at the electrode-electrolyte interface (Dantas et al., 2014). A similar trend was observed in the cyclic voltammetric responses for increasing concentrations of glucose (Figure 3B). As observed earlier in cyclic voltammetry, the net charge was found to increase with increasing concentrations of glucose (Figure 3C).

The GCE/CNT-GR-GOx bioelectrode was able to detect glucose concentrations upto 21 mM. A good linearity was observed between 3 mM to 14 mM with a linear regression coefficient of 0.99 as shown in Figure 3B along with good sensitivity of 0.439 μA cm^{-2} mM^{-1}. The coefficient of variation calculated for the amperometric data in the concentration range 1-14mM was found to lie between 0.33 and 1.18% indicating the reproducibility of the measurements. Beyond 14 mM, a slight deviation from the linearity was observed. Physiological concentrations of glucose under normal metabolic conditions range between

3.9 mM to 7.8 mM. Under hyperglycemic conditions, the blood glucose levels increase to a maximum of 15 mM (Hai and Zou, 2015; Li et al., 2015; Masur et al., 2011). Thus, the fabricated sensor has the range of detection that can be useful for determination of physiological concentrations of glucose.

The limits of detection and quantification were calculated by using the following formulae:

Limit of detection (LOD) = $\frac{[3.3xSD]}{Slope}$

Limit of quantification (LOQ) =$\frac{[10xSD]}{Slope}$

where SD is standard deviation. The LOD for the developed biosensor was found to be 2.99 µM and LOQ was 9.88 µM.

A plot of net current versus substrate concentration was obtained for calibration of the GCE/CNT-GR-GOx biosensor. The apparent Michaelis–Menten constant (K_M) and maximum net current (I_{max}) values were identified using the Hill plot (Figure 3D). The K_M was found to be 13.06 mM L^{-1} and I_{max} was determined to be 12.59 µA, which indicates the strong affinity between the GCE/CNT-GR-GOx and glucose. The GCE/CNT-GR-GOx biosensor demonstrated an efficiency of 45.5% calculated using the formula:

$$Biosensor\ efficiency = \frac{Practical\ sensitivity}{theoretical\ sensitivity} * 100$$

where,

$$\text{Theoretical sensitivity} = \frac{\text{Imax}}{\text{Km}} = 0.964$$

$$\text{Practical sensitivity} = \text{slope of the working electrode} = 0.439$$

The sensing characteristics of the designed biosensor were compared with previous reports employing different interface materials are summarized in Supplementary Table 2. It is evident from the comparison that the biosensor reported in this study exhibits superior sensitivity and wide range of detection. The response time of the sensor was also found to be rapid and was found from amperometric studies to be <4 seconds.

3.2.c. Effect of pH

In the case of GOx, direct electron transfer occurs at the interior FAD centre during the redox reaction. Therefore, the pH of the electrolytic solution will affect the redox potential of the reaction (Katz et al., 1999). To investigate the pH dependency of the peak potential, cyclic voltammograms were recorded at different pH and the results are presented in supplementary Figure 4. It was observed that the increase in the pH resulted in a shift of the peak potential towards negative potential as reported earlier (Kang et al., 2009). At pH 4, the oxidation peak was observed at -0.15 V, which shifted to -0.47 V at pH 7.4 and -0.55V at pH 9. Literature reports have shown that the optimum pH range for GOx is between 4 and 7.4 and the enzyme is stable up to pH 8. GOx has been found to be most active around pH 5 – 5.5 and hence it is observed that the oxidation peak occurs at much lower potentials in acidic pH. However, as the physiological pH is 7.4, all trials were carried out at this pH (Chen and Dong, 2003; Janegitz et al., 2011; Wang et al., 2011).

3.2.d. Precision

Inter and intra assays were performed to check the reproducibility and repeatability of the GCE/CNT-GR-GOx biosensor in the presence of 1 mM of glucose in PBS at pH 7.4. Inter-assay was performed using the same electrode for 10 measurements and the intra-assay was performed using three different electrodes for 4 measurements. The results obtained were analyzed using relative standard deviation (RSD). The RSD of the inter-assay was found to be 0.42% and intra-assay was 2.76%. These results confirmed that the electrode fabrication process and the immobilization of the enzyme on the electrode were reproducible.

3.2.e. Stability

Stability of the GCE/CNT-GR-GOx biosensor was checked in dry and wet conditions. The wet stability of the fabricated electrode was monitored by storing the modified same in PBS

and for dry stability assessment, the electrode was stored at -4^{o}C. Cyclic voltammetry was performed for a period of 40 days. 80% of the peak current was retained for the electrode stored at -4^{o} C for a period of 30 days. In the case of the electrode stored in PBS, 72% current was retained for 25days after which the peak current reduced significantly. These results confirm that the electrode exhibits reasonable stability in both storage conditions. The stability of the electrode was calculated using the equation.

$$\% \textbf{ Stability} = \mathbf{100} - \left[\frac{\{\mathbf{In} - \mathbf{Io}\}}{\mathbf{Io}}\right] \mathbf{x\ 100}$$

where, I_o is the current obtained at the first day and I_n is the current obtained at n^{th} day.

3.2.f. Interference study

To evaluate the specificity of the GCE/CNT-GR-GOx biosensor, amperometry was performed in the presence of different common interfering substrates at 1 mM each. It was observed that the biosensor was highly selective towards glucose and it did not respond significantly for other oxidized species such as uric acid, ascorbic acid and citric acid present in the human blood (Hai and Zou, 2015; Ye et al., 2013). Additionally, acetaminophen is a major interferent for glucose. The presence of 1 mole of acetaminophen has been reported to result in erroneous results with a reduction of up to 4 moles of glucose from the actual values (Chen and Dong, 2003; Kang et al., 2009; Suneesh et al., 2013). Therefore, we have also investigated the response of the developed biosensor towards acetaminophen. The results confirm that the GCE/CNT-GR-GOx biosensor is highly specific for glucose and can perform without being affected by potential interferents during real time analysis. Amperometric detection of potential interferents is shown in Supplementary Figure 5.

3.3. Application of the biosensor to determine cancer cell proliferation

Cells utilize glucose as a substrate for their metabolic activities and enhanced glucose utilization is a hallmark of an increased number of cells and therefore can serve as a method for monitoring the proliferation rate. The fabricated glucose sensor was employed to monitor the time-dependent glucose utilization of MiaPaCa-2 pancreatic cancer cells up to a period of 12 h. The cell culture medium was withdrawn from the well plates at pre-

determined time points and amperometry was performed at -0.45 V in PBS at pH 7.4 to quantify the glucose levels. The observed currents values were used to determine the concentration of glucose using a standard graph and the glucose utilization results are shown in Figure 4. Conventional biochemical method to monitor cell proliferation, namely Alamar blue assay, was also employed for comparison and the results are shown in Figure 4. Alamar blue assay is based on the conversion of the blue non-fluorescent resazurin to red fluorescent resarufin by metabolically active cells.

It is observed from the Figure 4 that both methods confirm an increase in the cell proliferation with time. As the cells proliferate, the demand for glucose increases, resulting in enhanced glucose consumption. The values showed that the cancer cells utilized more amount of glucose with respect to their proliferation (Figure 4B). Similar trend was observed with the Alamar blue proliferation assay also (Figure 4A). A negative correlation between cell density and glucose utilization is observed at the initial time points while at 12 h, a positive correlation is obtained between cell density and glucose utilization (Figure 4 C). This change in the trend may be attributed to the metabolic activity of a cell, which depends on numerous factors that include cell size, cell type and cell density (Dolfi et al., 2013). At low cell densities, the driving force for increasing cell numbers is high and therefore the cells exhibit greater metabolic activity while at higher cell densities, the driving force towards proliferation is slowed down and hence the glucose utilization tends to plateau off. Further, metabolically quiescent cells also display a basal level of glucose utilization. But, the Alamar blue assay depends upon the expression levels of mitochondrial reductase, cytochromes, NADPH and NADH reductases in the cells for transformation of resazurin to resarufin (Rampersad, 2012) . These levels can fluctuate in metabolically active and quiescent cells leading to the discrepancy in the values. Moreover, the conventional dye based assays can lead to errors in pipetting as well as quenching of the fluorescence emission by flavin reductase and other reductases and hence there is a degree of unreliability in the values especially at high cell densities. But, the use of the electrochemical biosensor can overcome these limitations and offer an effective alternate method for rapid determination of cell proliferation.

As glucose measurements using the fabricated sensor are quicker when compared to conventional biochemical assays, it can be used as a rapid method to monitor proliferation of cells. The glucose biosensor can also be used for rapid time-dependent monitoring of the cell proliferation in the same system, unlike the dye-based assays. In order to evaluate the accuracy of the glucose measurement by the fabricated sensor, the glucose levels of the medium were also determined using a commercial glucose sensor. The comparison of the results obtained from the fabricated glucose biosensor and commercial glucometer are presented in Table 1. The results revealed that the designed glucose biosensor are similar to those obtained from the commercial glucometer thereby confirming the precision and accuracy of the biosensor fabricated in the present work.

Further, the fabricated biosensor was employed for the estimation of cell proliferation and the cell numbers predicted based on glucose utilization were compared with the cell numbers obtained through conventional cell counting using hemocytometer. In the present study, different cell densities were employed for various trials and the results are shown in Figure 5A. It is observed that the glucose utilization increased with increasing cell numbers. The biphasic increase observed in the plot between cell number and glucose utilization was similar to the typical growth curve reported for cells. This standard plot was then employed to estimate cell numbers in independent experiments using glucose utilization values.

MiaPaCa2 cancer cells were cultured over a period of 10 days and the unutilized glucose was measured at different time points from the spent medium using the sensor. Independently, the cells were also counted using hemocytometer for comparison. The glucose utilization values determined using the fabricated sensor was converted in to cell numbers based on the standard graph. The comparison between the results obtained through glucose measurements and conventional hemocytometer are shown in Figure 5B. Glucose utilization values, predicted cell number and counted cell numbers are presented in Supplementary Table 3. The results of both the experiments showed a deviation less than 10%. The coefficient of variation for the glucose utilization values were found to be in the range 0.27 to 0.80%. It is evident from our results that the fabricated glucose biosensor can be used to predict the number of cells. Apart from being time-consuming, conventional

cell counting can lead to both positive and negative errors due to improper mixing, uneven dispersion of cells, under-counting or over-counting of cells, improper staining of the dye, etc. These problems can easily be overcome by employing the glucose sensor. Hence, this glucose biosensor can be explored as an effective tool to estimate the rate of proliferation of cells.

4. **Concluding remarks**

The present study reports the successful design and development of an electrochemical biosensor with hybrid nano-interface for the determination of glucose. The sensor characteristics reveal a wide range of detection up to 21 mM apart from rapid response of <4s and high sensitivity. This biosensor was successfully demonstrated to quantify glucose utilization in cancer cells as a novel method to monitor the proliferation rate. The use of electrochemical method for detection overcomes many of the limitations encountered in the conventional dye-based biochemical assays currently employed for measuring proliferation rates. Hence, we believe that this biosensor can be employed as a diagnostic tool for estimating the growth rate of cancer cells as well as determine the cytotoxic effects of therapeutic entities on the cancer cell proliferation.

Acknowledgements

Sasya Madhurantakam is thankful to DST for INSPIRE fellowship (DST/IF/120812). The authors wish to acknowledge Department of Science & Technology for providing cell culture facility through DST-FIST programme (SR/FST/LSI-453/2010). Authors are also thankful to SASTRA University for infrastructural and financial support.

Bokobza, L., Zhang, J., 2012. Raman spectroscopic characterization of multiwall carbon nanotubes and of composites. Express Polym. Lett. 6, 601–608. doi:10.3144/expresspolymlett.2012.63

Chen, X., Dong, S., 2003. Sol-gel-derived titanium oxide/copolymer composite based glucose biosensor. Biosens. Bioelectron. 18, 999–1004. doi:10.1016/S0956-5663(02)00221-X

Childres, I., Jauregui, L., Park, W., Cao, H., Chen, Y., 2013. Raman Spectroscopy of Graphene and Related Materials. New Dev. Phot. Mater. Res. 1–20. doi:10.1016/B978-0-444-53175-9.00016-7

Coller, H.A., Belfiore, A., Malaguarnera, R., Korzeniewski, C., Callewaert, D.M., Fischer, D., Li, Y., Ahlemeyer, B., Krieglstein, J., Kissel, T., Denizot, F., Lang, R., Frasca, F., Pandini, G., Scalia, P., Sciacca, L., Mineo, R., Costantino, A., Goldfine, I.D., Belfiore, A., Vigneri, R., Nakayama, G.R., Caton, M.C., Nova, M.P., Parandoosh, Z., Legrand, C., Bour, J.M., Jacob, C., Capiaumont, J., Martial, A., Marc, A., Wudtke, M., Kretzmer, G., Demangel, C., Duval, D., Hache, J., O'Brian,J.,Wilson,I.,Orton,T.,Pognan, F., Weyermann, J., Lochmann, D., Zimmer, A., van de Loosdrecht, A.A., Beelen, R.H., Ossenkoppele, G.J., Broekhoven, M.G., Langenhuijsen, M.M., Kulldorff, M., McShane, L.M., Schatzkin, A., Freedman, L.S., Wargovich, M.J., Woods, C., Purewal, M., Burt, R.W., Lawson, M., Mateski, D.J., Lanza, E., Corle, D.K., O'Brien, B., Moler, J., Mosmann, T., Manuscript, A., Borra, R.C., Lotufo, M.A., Gagioti, S.M., Barros, F.D.M., Andrade, P.M., Al-Nasiry, S., Hanssens, M., Luyten, C., Pijnenborg, R., Rampersad, S.N., Skehan, P., Storeng, R., Scudiero, D., Monks, A., McMahon, J., Vistica, D., Warren, J.T., Bokesch, H., Kenney, S., Boyd, M.R., Griss, T., Vincent, E.E., Egnatchik, R., Chen, J., Ma, E.H., Faubert, B., Viollet, B., DeBerardinis, R.J., Jones, R.G., Vijayakumar, S.N., Sethuraman, S., Krishnan, U.M., Papa, V., Gliozzo, B., Clark, G.M., McGuire, W.L., Moore, D., Fujita-Yamaguchi, Y., Vigneri, R., Goldfine, I.D., Pezzino, V., Zhi-Jun, Y., Sriranganathan, N., Vaught, T., Arastu, S.K., Ahmed, S. a, 2015. New colorimetric cytotoxicity assay for anticancer-drug screening. J. Immunol. Methods 53, 1304–1309. doi:10.1039/C5RA06505D

Dantas, L.M.F., Castro, P.S., Peña, R.C., Bertotti, M., 2014. Amperometric determination of hydrogen peroxide using a copper microelectrode. Anal. Methods 6, 2112. doi:10.1039/c3ay41980k

Dolfi, S.C., Chan, L.L.-Y., Qiu, J., Tedeschi, P.M., Bertino, J.R., Hirshfield, K.M., Oltvai, Z.N., Vazquez, A., 2013. The metabolic demands of cancer cells are coupled to their size and protein synthesis rates. Cancer Metab. 1, 20. doi:10.1186/2049-3002-1-20

Du, J., Zhao, L., Zeng, Y., Zhang, L., Li, F., Liu, P., Liu, C., 2011. Comparison of electrical properties between multi-walled carbon nanotube and graphene nanosheet/high density polyethylene composites with a segregated network structure. Carbon N. Y. 49, 1094–1100. doi:10.1016/j.carbon.2010.11.013

Felix, S., Kollu, P., Raghupathy, B.P.C., 2014. Electrocatalytic activity of Cu 2 O nanocubes-based electrode 126, 25–32.

Fu, Y., Liang, F., Tian, H., Hu, J., 2014. Nonenzymatic glucose sensor based on ITO electrode modified with gold nanoparticles by ion implantation. Electrochim. Acta 120, 314–318. doi:10.1016/j.electacta.2013.12.082

Gopalan, A.I., Lee, K.P., Ragupathy, D., Lee, S.H., Lee, J.W., 2009. An electrochemical glucose biosensor exploiting a polyaniline grafted multiwalled carbon nanotube/perfluorosulfonate ionomer-silica nanocomposite. Biomaterials 30, 5999–6005. doi:10.1016/j.biomaterials.2009.07.047

Griss, T., Vincent, E.E., Egnatchik, R., Chen, J., Ma, E.H., Faubert, B., Viollet, B., DeBerardinis, R.J., Jones, R.G., 2015. Metformin Antagonizes Cancer Cell Proliferation by Suppressing Mitochondrial-Dependent Biosynthesis. PLoS Biol. 13, 1–23. doi:10.1371/journal.pbio.1002309

Guascito, M.R., Chirizzi, D., Picca, R.A., Mazzotta, E., Malitesta, C., 2011. Ag nanoparticles capped by a nontoxic polymer: Electrochemical and spectroscopic characterization of a novel nanomaterial for glucose detection. Mater. Sci. Eng. C 31, 606–611. doi:10.1016/j.msec.2010.11.022

Guo, C.X., Li, C.M., 2010. Direct electron transfer of glucose oxidase and biosensing of glucose on hollow sphere-nanostructured conducting polymer/metal oxide composite. Phys. Chem. Chem. Phys. 12, 12153–12159. doi:10.1039/c0cp00378f

Hai, B., Zou, Y., 2015. Carbon cloth supported NiAl-layered double hydroxides for flexible application and highly sensitive electrochemical sensors. Sensors Actuators B Chem. 208, 143–150. doi:10.1016/j.snb.2014.11.022

Hu, H., Feng, M., Zhan, H., 2015. A glucose biosensor based on partially unzipped carbon nanotubes. Talanta 141, 66–72. doi:10.1016/j.talanta.2015.03.057

Hyun, K., Won, S., Koh, W., Kwon, Y., 2014. ScienceDirect Direct electrochemistry of glucose oxidase immobilized on carbon nanotube for improving glucose sensing. Int. J. Hydrogen Energy 40, 2199–2206. doi:10.1016/j.ijhydene.2014.12.019

Janegitz, B.C., Pauliukaite, R., Ghica, M.E., Brett, C.M. a., Fatibello-Filho, O., 2011. Direct electron transfer of glucose oxidase at glassy carbon electrode modified with functionalized carbon nanotubes within a dihexadecylphosphate film. Sensors Actuators B Chem. 158, 411–417. doi:10.1016/j.snb.2011.06.048

Jang, M., Kim, S.S., Lee, J., 2013. Cancer cell metabolism: implications for therapeutic targets. Exp. Mol. Med. 45, e45. doi:10.1038/emm.2013.85

Kang, X., Mai, Z., Zou, X., Cai, P., Mo, J., 2007. A novel glucose biosensor based on immobilization of glucose oxidase in chitosan on a glassy carbon electrode modified with gold–platinum alloy nanoparticles/multiwall carbon nanotubes. Anal. Biochem. 369, 71–79. doi:10.1016/j.ab.2007.07.005

Kang, X., Wang, J., Wu, H., Aksay, I. a., Liu, J., Lin, Y., 2009. Glucose Oxidase–graphene–chitosan modified electrode for direct electrochemistry and glucose sensing. Biosens. Bioelectron. 25, 901–905. doi:10.1016/j.bios.2009.09.004

Katz, E., Riklin, A., Heleg-Shabtai, V., Willner, I., Bückmann, A.F., 1999. Glucose oxidase electrodes via reconstitution of the apo-enzyme: Tailoring of novel glucose biosensors. Anal. Chim. Acta 385, 45–58. doi:10.1016/S0003-2670(98)00688-6

Klement, R.J., Kämmerer, U., 2011. Is there a role for carbohydrate restriction in the treatment and prevention of cancer? Nutr. Metab. (Lond). 8, 75. doi:10.1186/1743-7075-8-75

Korzeniewski, C., Callewaert, D.M., 1983. An enzyme-release assay for natural cytotoxicity. J. Immunol. Methods 64, 313–320. doi:10.1016/0022-1759(83)90438-6

Kulldorff, M., McShane, L.M., Schatzkin, A., Freedman, L.S., Wargovich, M.J., Woods, C., Purewal, M., Burt, R.W., Lawson, M., Mateski, D.J., Lanza, E., Corle, D.K., O'Brien, B., Moler, J., 2000. Measuring cell proliferation in the rectal mucosa. J. Clin. Epidemiol. 53, 875–883. doi:10.1016/S0895-4356(99)00180-8

Kumar, V., Shorie, M., Ganguli, A.K., Sabherwal, P., 2015. Graphene-CNT nanohybrid aptasensor for label free detection of cardiac biomarker myoglobin. Biosens. Bioelectron. 72, 56–60. doi:10.1016/j.bios.2015.04.089

Lei, Y., Yan, X., Luo, N., Song, Y., Zhang, Y., 2010. ZnO nanotetrapod network as the adsorption layer for the improvement of glucose detection via multiterminal electron-exchange. Colloids Surfaces A Physicochem. Eng. Asp. 361, 169–173. doi:10.1016/j.colsurfa.2010.03.029

Li, H., Guo, C.-Y., Xu, C.-L., 2015. A highly sensitive non-enzymatic glucose sensor based on bimetallic Cu–Ag superstructures. Biosens. Bioelectron. 63, 339–346. doi:10.1016/j.bios.2014.07.061

Li, S.-J., Xia, N., Lv, X.-L., Zhao, M.-M., Yuan, B.-Q., Pang, H., 2014. A facile one-step electrochemical synthesis of graphene/NiO nanocomposites as efficient electrocatalyst for glucose and methanol. Sensors Actuators B Chem. 190, 809–817. doi:10.1016/j.snb.2013.09.047

Liu, S., Ju, H., 2003. Reagentless glucose biosensor based on direct electron transfer of glucose oxidase immobilized on colloidal gold modified carbon paste electrode. Biosens. Bioelectron. 19, 177–183. doi:10.1016/S0956-5663(03)00172-6

Lyons, M.E.G., Keeley, G.P., 2006. The Redox Behaviour of Randomly Dispersed Single Walled Carbon Nanotubes both in the Absence and in the Presence of Adsorbed Glucose Oxidase. Sensors 6, 1791–1826. doi:10.3390/s6121791

Malitesta, C., Guascito, M.R., Mazzotta, E., Siciliano, T., Tepore, A., 2013. Copper nanoparticles/poly-3-methylthiophene composite: Synthesis, characterization and catalytic application to enzyme-less glucose detecting. Sensors Actuators B Chem. 184, 70–77. doi:10.1016/j.snb.2013.04.001

Marinho, B., Ghislandi, M., Tkalya, E., Koning, C.E., de With, G., 2012. Electrical conductivity of compacts of graphene, multi-wall carbon nanotubes, carbon black, and graphite powder. Powder Technol. 221, 351–358. doi:10.1016/j.powtec.2012.01.024

Masur, K., Vetter, C., Hinz, A., Tomas, N., Henrich, H., Niggemann, B., Zänker, K.S., 2011. Diabetogenic glucose and insulin concentrations modulate transcriptom and protein levels involved in tumour cell migration, adhesion and proliferation. Br. J. Cancer 104, 345–352. doi:10.1038/sj.bjc.6606050

Panky, S., Thandavan, K., Sivalingam, D., Sethuraman, S., Krishnan, U.M., Jeyaprakash, B.G.,

Rayappan, J.B.B., 2013. Lipase immobilized on nanostructured cerium oxide thin film coated on transparent conducting oxide electrode for butyrin sensing. Mater. Chem. Phys. 137, 892–897. doi:10.1016/j.matchemphys.2012.10.031

Periasamy, A.P., Chang, Y.-J., Chen, S.-M., 2011. Amperometric glucose sensor based on glucose oxidase immobilized on gelatin-multiwalled carbon nanotube modified glassy carbon electrode. Bioelectrochemistry 80, 114–120. doi:10.1016/j.bioelechem.2010.06.009

Rampersad, S.N., 2012. Multiple applications of alamar blue as an indicator of metabolic function and cellular health in cell viability bioassays. Sensors (Switzerland) 12, 12347–12360. doi:10.3390/s120912347

Si, P., Ding, S., Yuan, J., Lou, X.W., Kim, D.H., 2011. Hierarchically structured one-dimensional TiO2 for protein immobilization, direct electrochemistry, and mediator-free glucose sensing. ACS Nano 5, 7617–7626. doi:10.1021/nn202714c

Skehan, P., Storeng, R., Scudiero, D., Monks, A., McMahon, J., Vistica, D., Warren, J.T., Bokesch, H., Kenney, S., Boyd, M.R., 1990. New colorimetric cytotoxicity assay for anticancer-drug screening. J. Natl. Cancer Inst. 82, 1107–1112. doi:10.1093/jnci/82.13.1107

Song, H., Cai, K., Wang, J., Shen, S., 2016. Influence of polymerization method on the thermoelectric properties of multi-walled carbon nanotubes/polypyrrole composites. Synth. Met. 211, 58–65. doi:10.1016/j.synthmet.2015.11.013

Sun, J.-Y., Huang, K.-J., Fan, Y., Wu, Z.-W., Li, D.-D., 2011. Glassy carbon electrode modified with a film composed of Ni(II), quercetin and graphene for enzyme-less sensing of glucose. Microchim. Acta 174, 289–294. doi:10.1007/s00604-011-0625-0

Suneesh, P.V., Chandhini, K., Ramachandran, T., Nair, B.G., Satheesh Babu, T.G., 2013. Tantalum oxide honeycomb architectures for the development of a non-enzymatic glucose sensor with wide detection range. Biosens. Bioelectron. 50, 472–477. doi:10.1016/j.bios.2013.07.007

Wang, Y., Liu, L., Li, M., Xu, S., Gao, F., 2011. Multifunctional carbon nanotubes for direct electrochemistry of glucose oxidase and glucose bioassay. Biosens. Bioelectron. 30, 107–111. doi:10.1016/j.bios.2011.08.038

Wu, X., Zhao, F., Varcoe, J.R., Thumser, A.E., Avignone-Rossa, C., Slade, R.C.T., 2009. Direct electron transfer of glucose oxidase immobilized in an ionic liquid reconstituted cellulose-carbon nanotube matrix. Bioelectrochemistry 77, 64–68. doi:10.1016/j.bioelechem.2009.05.008

Yang, J., Lee, H., Cho, M., Nam, J., Lee, Y., 2012. Nonenzymatic cholesterol sensor based on spontaneous deposition of platinum nanoparticles on layer-by-layer assembled CNT thin film. Sensors Actuators, B Chem. 171-172, 374–379. doi:10.1016/j.snb.2012.04.070

Yang, P., Tong, X., Wang, G., Gao, Z., Guo, X., Qin, Y., 2015. NiO/SiC Nanocomposite Prepared by Atomic Layer Deposition Used as a Novel Electrocatalyst for Nonenzymatic Glucose Sensing. ACS Appl. Mater. Interfaces 7, 4772–4777. doi:10.1021/am508508m

Ye, D., Liang, G., Li, H., Luo, J., Zhang, S., Chen, H., Kong, J., 2013. A novel nonenzymatic sensor based on CuO nanoneedle/graphene/carbon nanofiber modified electrode for probing glucose in saliva. Talanta 116, 223–230. doi:10.1016/j.talanta.2013.04.008

Zhang, H., Meng, Z., Wang, Q., Zheng, J., 2011. A novel glucose biosensor based on direct electrochemistry of glucose oxidase incorporated in biomediated gold nanoparticles–carbon nanotubes composite film. Sensors Actuators B Chem. 158, 23–27. doi:10.1016/j.snb.2011.04.057

Zhang, X., Liao, Q., Chu, M., Liu, S., Zhang, Y., 2014. Structure effect on graphene-modified enzyme electrode glucose sensors. Biosens. Bioelectron. 52, 281–287. doi:10.1016/j.bios.2013.07.022

Zhao, J., Chen, G., Zhu, L., Li, G., 2011. Graphene quantum dots-based platform for the fabrication of electrochemical biosensors. Electrochem. commun. 13, 31–33. doi:10.1016/j.elecom.2010.11.005

Zheng, J., 2012. Energy metabolism of cancer: Glycolysis versus oxidative phosphorylation (review). Oncol. Lett. 4, 1151–1157. doi:10.3892/ol.2012.928

Zhou, Y.-B., Liao, Z.-M., Wang, Y.-F., Duesberg, G.S., Xu, J., Fu, Q., Wu, X.-S., Yu, D.-P., 2010. Ion irradiation induced structural and electrical transition in graphene. J. Chem. Phys. 133, 234703. doi:10.1063/1.3518979

Zhu, J., Chen, X., Yang, W., 2010. A high performance electrochemical sensor for NADH based on graphite nanosheet modified electrode. Sensors Actuators B Chem. 150, 564–568. doi:10.1016/j.snb.2010.08.039

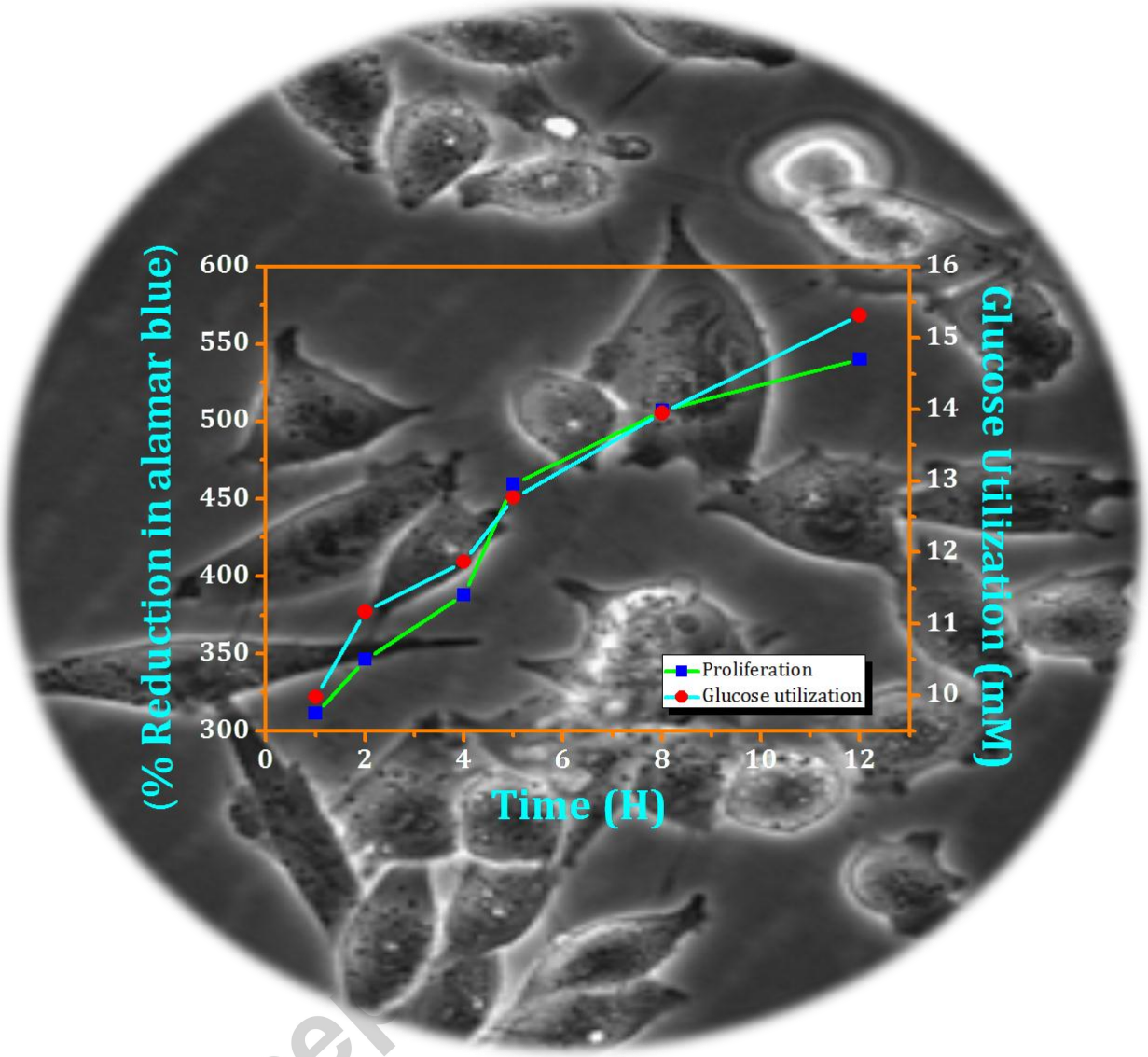

Figure 1: Scanning electron micrographs of CNTs (A), Graphene (B), both CNTs and Graphene without nafion(C) and with nafion (D), uniform distribution of GOx on the surface of CNT/GR/nafion at low (E) and high (F) resolution, (G) Raman modes of MWCNTs, graphene and MWCNTs-graphene composite.

Figure 2: (A) Cyclic voltammograms of different modified electrodes [A: MWCNTs; B: Graphene; C: MWCNT/GR; D: MWCNT/GR/GOx]; (B) Cyclic voltammopgrams MWCNT/GR/GOx in the absence and presence of 1mM glucose; (C) Schematic representation of reaction mechanism at the surface of the GCE/CNT-GR/GOx electrode; (D) Cyclic voltammogram of GCE/CNT-GR-GOx electrode in the presence of 1 mM of

glucose at different scan rates; (D) Plot of scan rate vs current; (E) Plot of square root of scan rate vs current; (F) Cyclic voltammograms of GCE/CNT-GR-GOx with increasing concentrations from 1mM to 7 mM glucose; (F) Plot of concentration vs current.

Figure 3: A) Amperometric pattern for the successive addition of 1 mM glucose from 1-21mM; B) liner plot of glucose concentration vs current; C) Shows the increase in the charge consumption with time; D) Hill plot using glucose concentration vs current.

Figure 4: A) Plot of % of proliferation with respect to time for various cell densities; B) plot of glucose utilization with respect to time for various cell densities; Comparison of % reduction in Alamar blue and glucose utilization with respect to various cell densities at different time points (C) 1h; (D) 4h; (E) 8h; (F) 12h.

Figure 5: A) Plot of number of cells vs glucose utilization B) Comparison of cell number counted using hemocytometer and predicted number of cells using glucose utilization.

Figure 1:

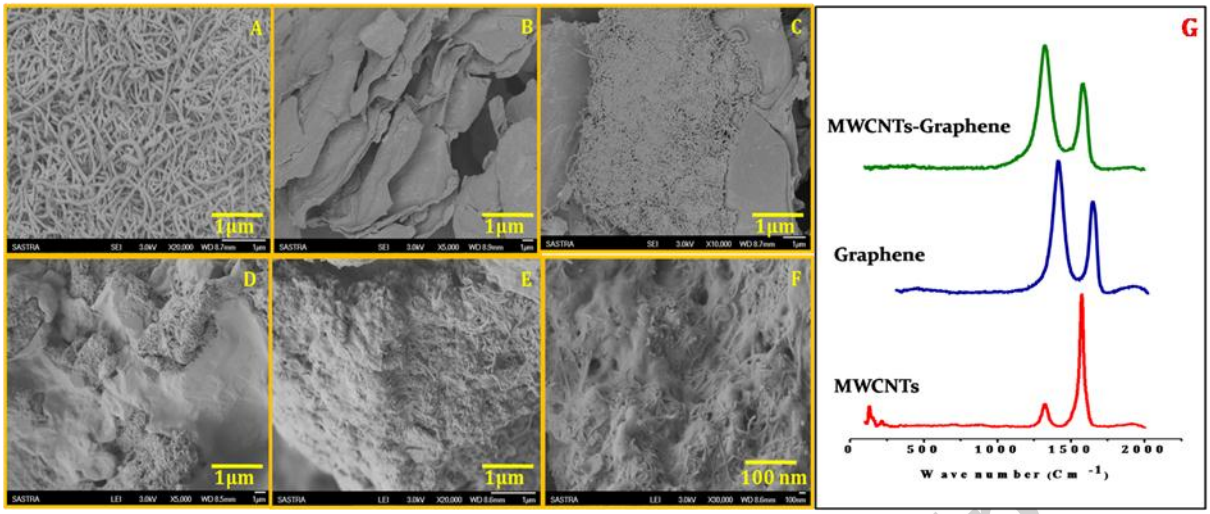

Figure 2:

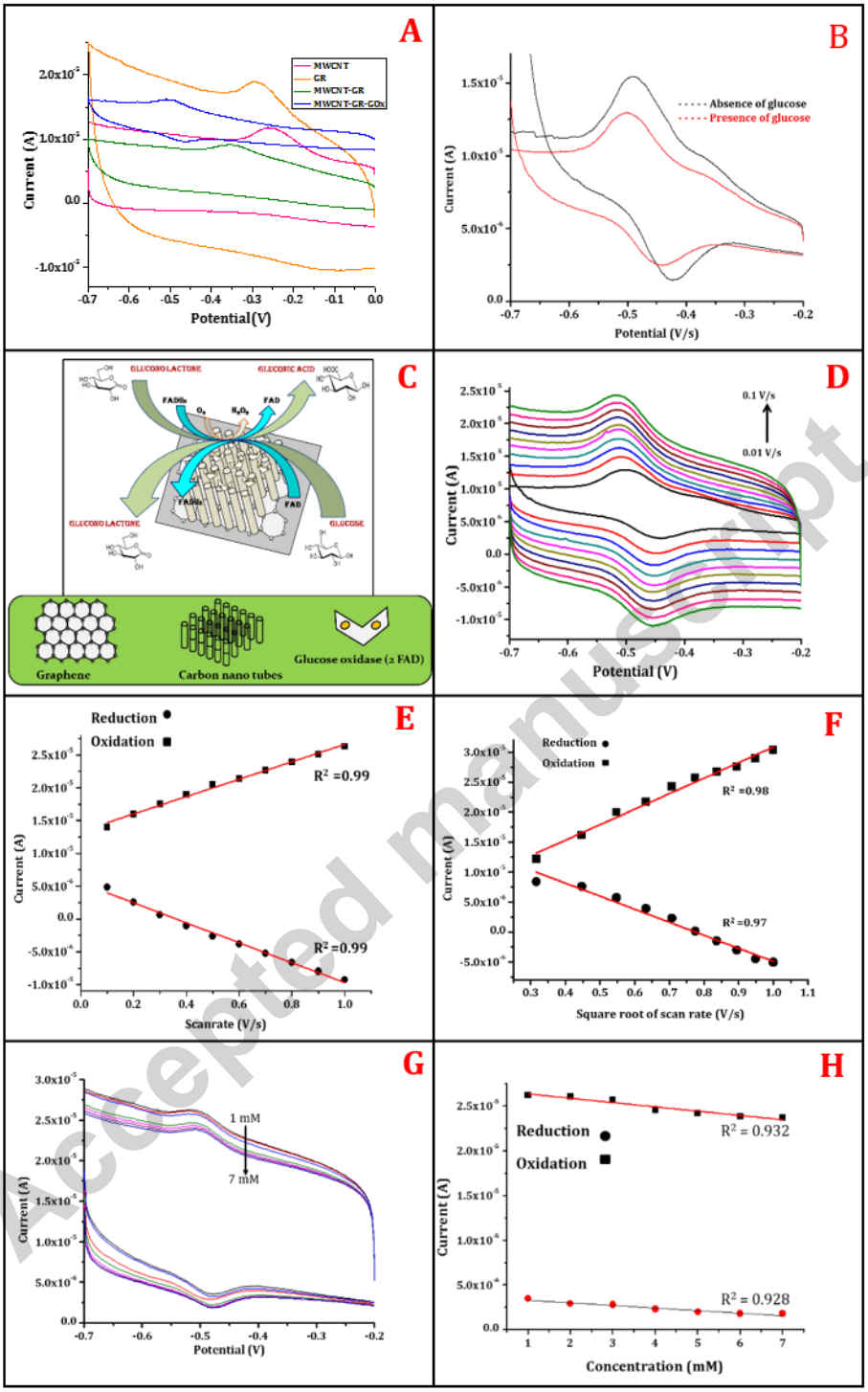
A
MWCNT
GR
MWCNT-GR
MWCNT-GR-GOx
Current (A)
Potential(V)
B
Absence of glucose
Presence of glucose
Current (A)
Potential (V/s)
C
GLUCONO LACTONE
GLUCONIC ACID
FADH2
O2
H2O2
FAD
GLUCONO LACTONE
GLUCOSE
Graphene
Carbon nano tubes
Glucose oxidase (2 FAD)
D
0.1 V/s
0.01 V/s
Current (A)
Potential (V)
E
Reduction
Oxidation
R² =0.99
R² =0.99
Current (A)
Scanrate (V/s)
F
Reduction
Oxidation
R² =0.98
R² =0.97
Current (A)
Square root of scan rate (V/s)
G
1 mM
7 mM
Current (A)
Potential (V)
H
Reduction
Oxidation
R² = 0.932
R² = 0.928
Current (A)
Concentration (mM)

Figure 3:

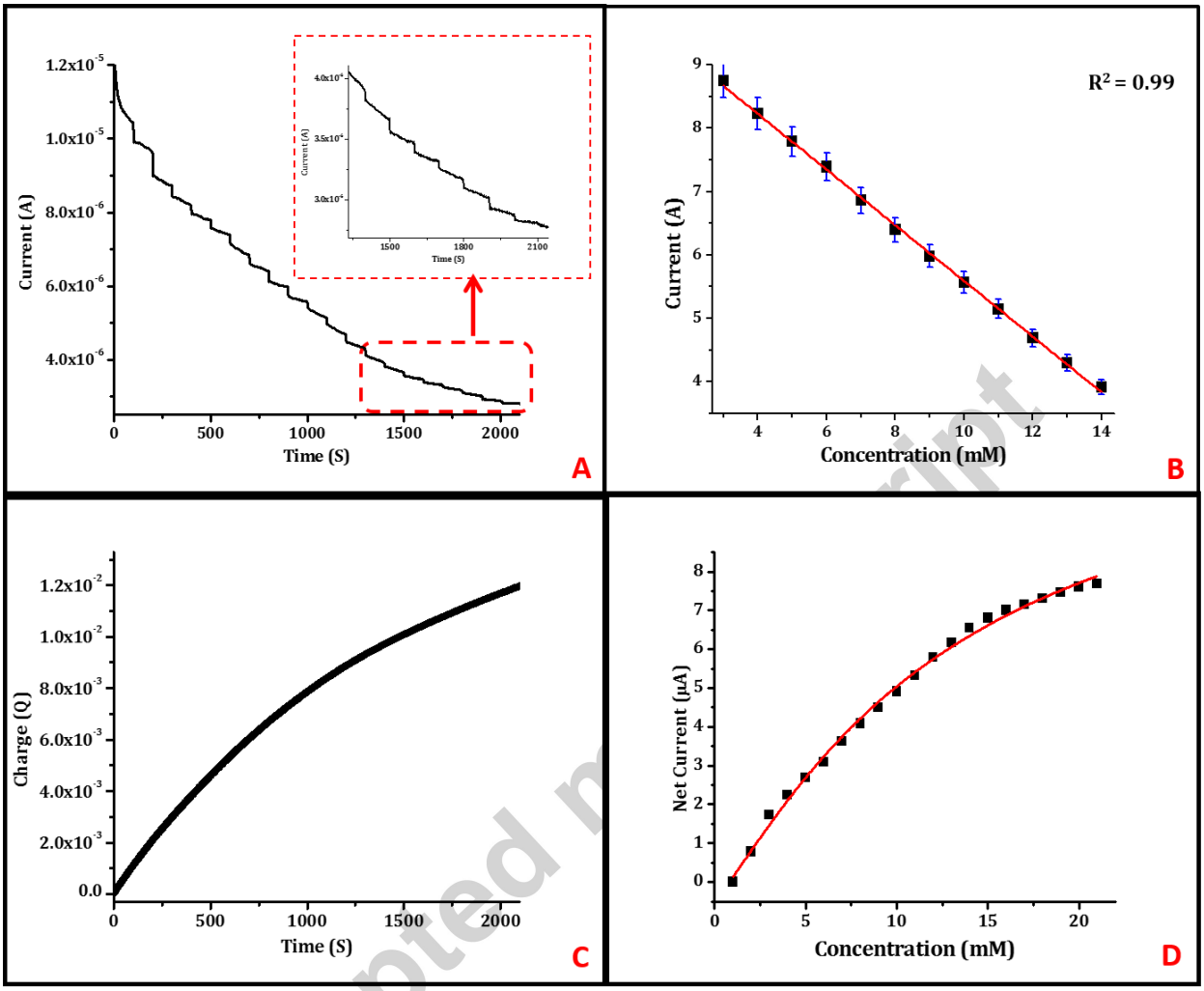

Figure 4:

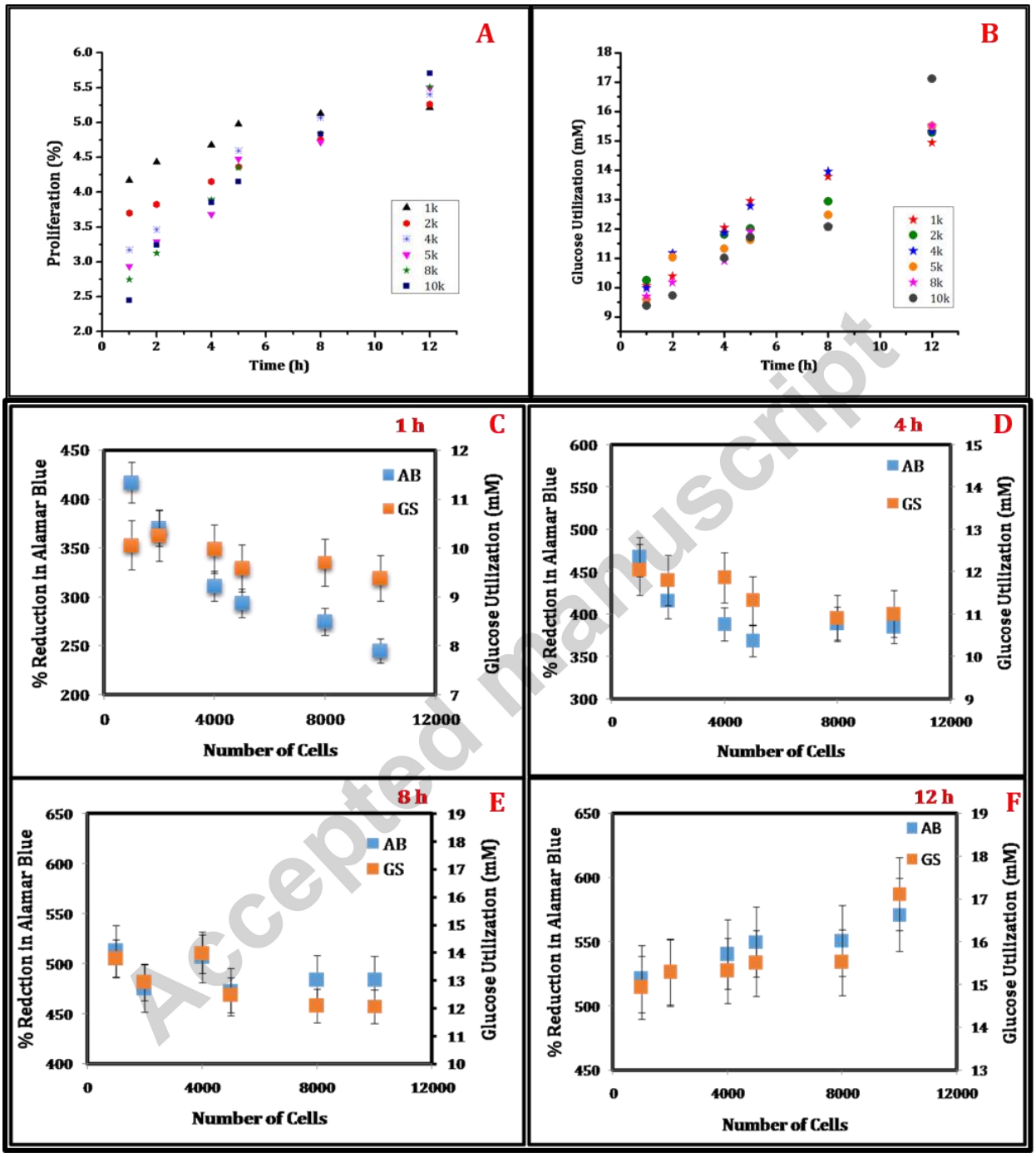

Figure 5:

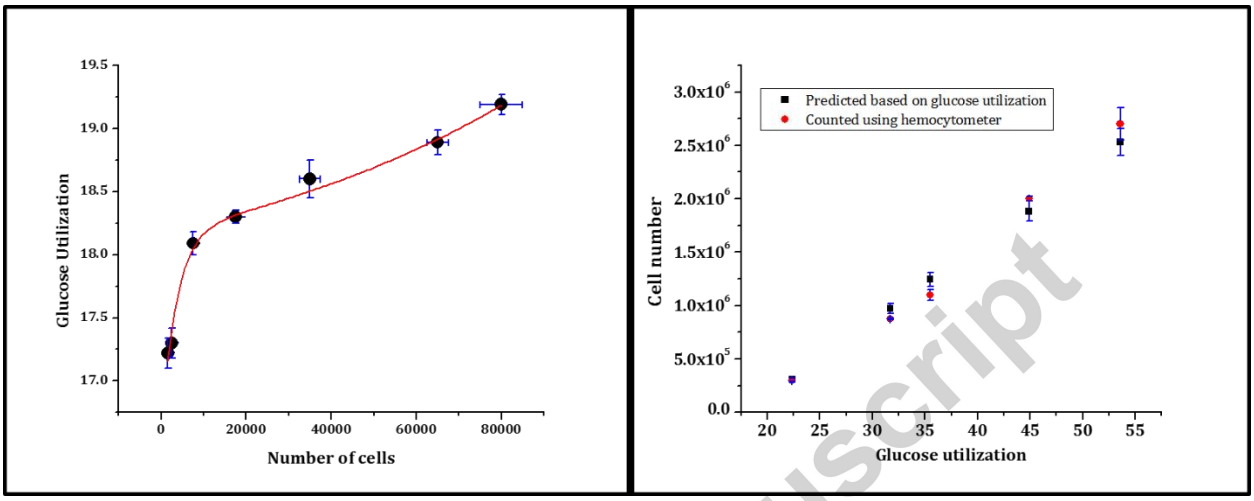

Table 1: Comparision of glucose utilization values obtained from the fabricated glucose biosensor and commercial glucometer.

	A= Amperometry				B = Commercial Glucometer							
Time (h)	**1**		**2**		**4**		**5**		**8**		**12**	
No. of cells	**A**	**B**	**A**	**B**	**A**	**B**	**A**	**B**	**A**	**B**	**A**	**B**
1k	14.94	14.84	14.6	14.81	12.95	13.2	12.05	12.65	11.22	11.54	10.68	10.26
2k	14.74	14.65	13.96	14.43	13.19	13.32	12.98	13.04	12.06	12.22	9.71	9.87
4k	15.02	15.26	13.82	14.26	13.13	13.15	12.32	13.32	11.04	12.21	9.68	9.43
5k	15.4	15.54	13.96	13.87	13.67	13.76	13.37	13.59	12.52	13.2	9.5	9.37
8k	15.29	15.42	14.82	14.7	14.09	14.43	13.09	14.09	12.92	13.1	9.48	9.15

10k	15.61	15.81	15.26	15.42	13.99	14.7	13.29	13.7	12.9	12.21	7.88	8.38

Highlights

- ✓ Carbon nanotube and graphene hybrid nano-interface was successfully employed for the development of electrochemical glucose sensor
- ✓ The sensor was used to determine proliferation of MiaPaCa-2 cancer cells based on utilization of glucose
- ✓ The results obtained from the amperometric technique were similar to the values obtained from a commercial glucometer
- ✓ Alamar blue assay was performed to check the proliferation rate of the cells and a good correlation was obtained between the proliferation rate and glucose utilization
- ✓ The developed biosensor may serve as a novel *in vitro* tool to rapidly quantify the proliferation rates of cancer cells in response to different treatment strategies